

MULTI-VIEW CLOUD-TOP HEIGHT AND WIND RETRIEVAL WITH PHOTOGRAMMETRIC METHODS: APPLICATION TO METEOSAT-8 HRV OBSERVATIONS

G. Seiz¹, A. Grün¹, S. Tjemkes² and R. Davies³

¹ Institute of Geodesy and Photogrammetry, ETHZ, CH-8093 Zuerich

² EUMETSAT

³ Jet Propulsion Laboratory

ABSTRACT

The height assignment of atmospheric motion vectors (AMV) is still an open issue. From the numerous height assignment techniques, each retrieval method has its own characteristics. The presented stereo-photogrammetric method has the advantage that it is only dependent on the geometry and therefore offers a completely independent height retrieval compared to the other methods. As polar-orbiting instrument, the Multi-angle Imaging SpectroRadiometer (MISR) onboard EOS-Terra is used. With its nine viewing angles, it offers simultaneous cloud-top height (CTH) and wind (CTW) retrieval from at least three non-symmetric cameras. The operational Meteosat satellites (M5, M7 and M8) allow geostationary stereo height retrievals within the overlap area over the Indian Ocean and East Africa. In addition to the M5/M7 combination, the new combination M5/M8 HRV is analyzed with our photogrammetric methods.

Two examples of coincident MISR, Meteosat-5, -7 and -8 HRV data over the Indian Ocean and East Africa are shown. The stereo-photogrammetric CTH and CTW results from MISR, Meteosat-5/-7 and Meteosat-5/-8 HRV are then compared with the operational NASA-JPL MISR L2TC product.

1. INTRODUCTION

Stereoscopy of clouds has a long tradition in meteorology (Hasler 1981). Stereo measurements have the advantage that they depend only on basic geometric relationships of observations of cloud features from at least two different viewing angles, while other cloud top height (CTH) estimation methods are dependent on the knowledge of additional cloud/atmosphere parameters like cloud emissivity, ambient temperature or lapse rate. From satellites, both geostationary and polar-orbiting sensors can be used in a number of configurations, as described in e.g. Fujita (1982), Campbell and Holmlund (2000), Yi et al. (2001).

The first stereo configuration with two Meteosat satellites was achieved with Meteosat-5 and Meteosat-7 over the Indian Ocean, since the Meteosat-5 satellite was placed at 63° E for the INDOEX project (Campbell and Holmlund 2000, Campbell and Holmlund 2004). With the installation of Meteosat-6 as rapid scanning geostationary satellite for the Mesoscale Alpine Programme (MAP) in autumn 1999 and operationally since September 2001, an additional Meteosat stereo configuration became available with a large overlap area over Europe. Unfortunately, this stereo configuration of Meteosat-6 and Meteosat-7 over Europe cannot be used for quantitative stereo analysis due to the small longitude difference and the low spatial resolution of the images. For the first satellite of the Meteosat Second Generation (MSG), Meteosat-8, the spatial resolution of channel 12, high-resolution visible (HRV), was increased significantly by about a factor 3, resulting in a spatial resolution at the sub-satellite point (SSP) of about 1.0 km. This new satellite, launched

in August 2002, offers the possibility of higher-resolution geostationary stereo retrievals in combination with Meteosat-5, which should then translate into more accurate stereo cloud-top heights. The only disadvantage of Meteosat-8 vs. Meteosat-7 for this purpose is the different scan period (i.e. 15 min vs. 30 min), so that there is a significant time difference between the Meteosat-5 and Meteosat-8 HRV image of 0 to ± 7.5 minutes, while the time difference between Meteosat-5 and Meteosat-7 is much smaller, 0 to ± 50 s, with small time differences for most parts except regions towards the image borders.

This paper extends the multi-view cloud-top height and motion retrievals described in Seiz and Baltasvias (2000), Seiz et al. (2001) and Seiz et al. (2003) to geostationary stereo height and motion retrieval, with special focus on the new Meteosat-8 HRV/ Meteosat-5 combination. Thereby, the main objective is to document the accuracy and limitations of the stereo height assignment using the Meteosat-8 HRV and the visible channels on Meteosat-5 or -7. It is a first step towards a more comprehensive intercomparison between the stereo height assignment and the more traditional methodologies implemented in the operational processing facility at Eumetsat, which are currently evaluated in a comparison study of various cloud height assignment methods (Fischer et al., 2004).

After a description of the data, methods and error sources, the cloud-top height and motion results from two target areas in December 2003, in coincidence with MISR, are shown. The results are then compared to the MISR CTH/CTW results based on L1B2 data and to the operational NASA-JPL MISR L2TC stereo CTH/CTW product.

2. DATA

2.1 Meteosat First Generation

Meteosat First Generation (MFG) is a series of spin-stabilized satellites which rotates at 100 revolutions per minute (i.e. 0.6 s per line) from South to North, providing a full disk image every 30 minutes. The S-N scan actually takes only 25 minutes, with 5 minutes spare time for a retrace of the scan mirror and to stabilize the satellite. The main payload of MFG is the Meteosat Visible and Infrared Imager (MVISIRI). This is a three channel radiometer with a channel in the visible (VIS; 0.4 - 1.1 μm), water vapour (WV; 5.7 - 7.1 μm) and infrared (IR; 10.5 - 12.5 μm) part of the spectrum. The VIS image consists of 5000 x 5000 pixels with 2.5 km resolution at the SSP, while a WV/IR image contains 2500 x 2500 pixels with 5.0 km resolution at the SSP.

In the present study, images by MVISIRI onboard Meteosat-5 and -7 were used, with a nominal SSP of 63° E and 0° longitude, respectively. Rectified MFG data were obtained from the Eumetsat archive in RECT2LP format, which includes the necessary information about the actual satellite position (at image start and image end) in the header.

2.2 Meteosat Second Generation

The Spinning Enhanced Visible and Infrared Radiometer (SEVIRI) is the main payload of the Meteosat Second Generation (MSG) satellites. Meteosat-8 is the first one of this series and is currently located at 3.4° W longitude. Its images are rectified to 0° nominal longitude during georectification. SEVIRI has 11 spectral channels with a sampling distance of 3.0 km and one channel (the High Resolution Visible HRV) with a sampling distance of 1.0 km.

The SEVIRI HRV channel covers only part of the hemisphere; furthermore, the upper and lower HRV segment can be shifted. For instance, Figure 1 shows the upper segment centered over Europe and the lower segment shifted to the Eastern edge. This configuration is optimal for our stereo CTH retrieval purpose, as it presents a nearly maximal overlap with Meteosat-5 (except for the upper-right corner in the upper segment), as illustrated in Figure 2.

Meteosat-8 data were provided in L1.5 native format. The actual pixel and line positions of the two HRV segments are listed in the trailer of the L1.5 native image files, within the field 'ActualL15CoverageHRV'. The satellite position for each cloud point was calculated from the orbit polynom and the mean line acquisition time information given in the L1.5 file.

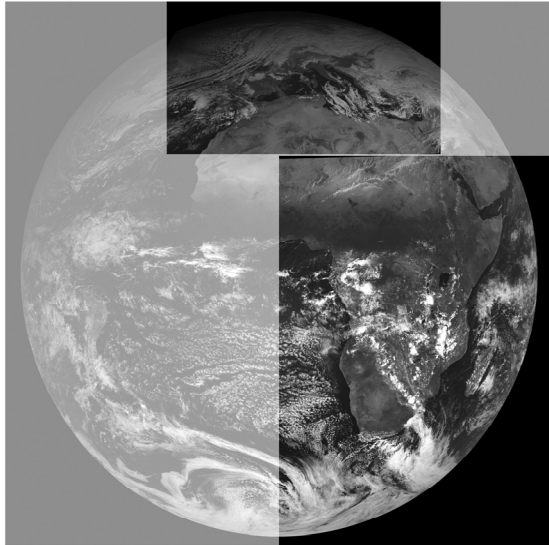


Figure 1. Upper and lower HRV segments, overlaid on the low-resolution visible channel.

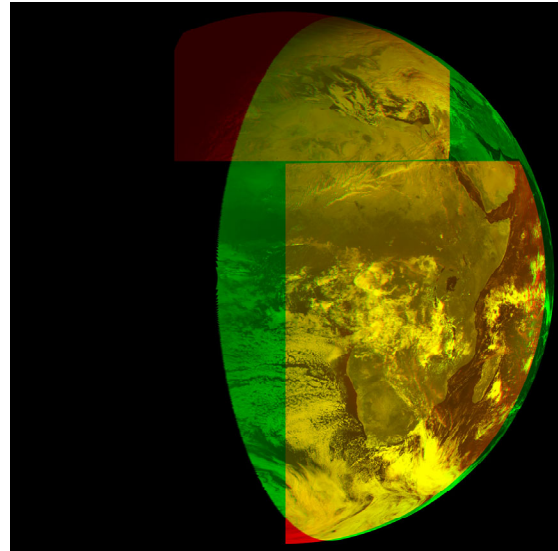


Figure 2. Anaglyph image of Meteosat-8 HRV (red) and Meteosat-5 (green) (red = left eye).

2.3 MISR

The Multi-angle Imaging SpectroRadiometer (MISR) was launched onboard the EOS AM-1 Terra spacecraft in December 1999. The orbit is sun-synchronous at a mean height of 705 km, with an inclination of 98.5° and an equatorial crossing time at about 10:30 am. The repeat cycle is 16 days. The MISR instrument consists of nine pushbroom cameras at different viewing angles: -70.5° (named DA), -60.0° (CA), -45.6° (BA), -26.1° (AA), 0.0° (AN), 26.1° (AF), 45.6° (BF), 60.0° (CF), and 70.5° (DF). The time delay between adjacent camera views is 45-60 seconds which results in a total delay between the DA and DF image of about 7 minutes. The four MISR spectral bands are centered at 446 (blue), 558 (green), 672 (red), and 866 nm (NIR). The data of the red band from all nine cameras and of the blue, green and NIR bands of the AN camera are saved in high-resolution, with a pixel size of 275×275 m; the data of the blue, green and NIR bands of the remaining eight cameras are stored in low-resolution, with a pixel size of 1.1×1.1 km.

The operational data products from NASA are described in Lewicki et al. (1999); the two products used for our investigations are the L1B2 Ellipsoid data (geolocated product) and the L2TC data (top-of-the-atmosphere/ cloud product) (Diner et al., 1999; Horvath and Davies, 2001; Horvath et al., 2002).

3. METHODS

3.1 Remapping to common grid

For the matching, the images should be remapped to a common projection, to avoid matching errors due to distortions. Remapping to either the Meteosat-5 or Meteosat-8 HRV projections is not optimal, as these projections are highly distorted towards the image borders. Recommended projections are e.g. the Universal Transversal Mercator (UTM) projection. In our developed remapping routine, any target grid and projection can be chosen. The remapping is then done by back-projection, i.e. each target pixel is back-projected into the original Meteosat image. The value for the target pixel is then calculated by cubic, bilinear or nearest neighbour interpolation, as chosen by the user.

To allow an optimal comparison with the MISR reference data, the Meteosat data were remapped to the MISR SOM grid of a specific MISR path. For the whole analysis, all images were remapped with cubic interpolation.

In a later stage, it would be better to start with the unrectified images and directly remap them to the common projection, to avoid loss of precision due to multiple resampling.

3.2 CTH/CTW retrieval

The main task in stereo CTH and CTW retrieval is the automatic identification of the same cloud features in the multiple views, the so-called 'matching'. Matching of near-simultaneous views from a multi-view polar-orbiting instrument (e.g. MISR) and matching/tracking of geostationary images (≤ 15 -minute time interval) can be treated with a similar processing chain (Figure 3). For both tasks, we apply the Multi-Photo Geometrically Constrained (MPGC) matching algorithm developed at our Institute (Baltsavias, 1991), which is based on Least-Squares-Matching (LSM) (Grün, 1985). The algorithm has already been tested on a number of ground-based multi-view CCD images of clouds as well as on satellite-based cloud images from ATSR2, MISR and ASTER (Seiz, 2003).

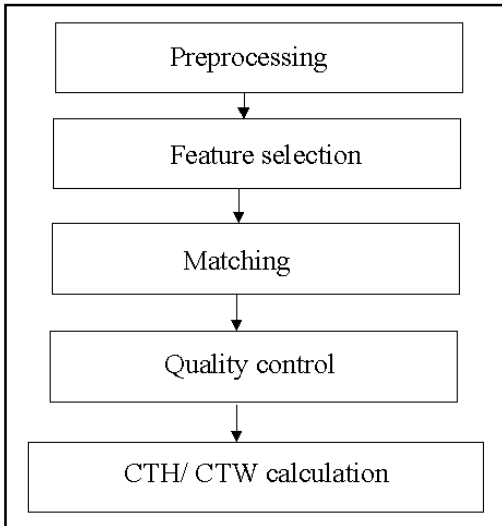


Figure 3. Overview of the processing steps for multi-view CTH/CTW retrieval.

The processing steps to derive stereo CTH and CTW are illustrated in Figure 3. For MISR, a hierarchical matching procedure with 4 pyramid levels was applied, as no a priori values of the cloud heights were given to the matching algorithm. Every pyramid level was enhanced and radiometrically equalized with a Wallis filter (Wallis, 1976). Points with good texture were then selected with an interest operator (Förstner and Gülch, 1987). After the MPGC matching, the matching solutions were quality-controlled with absolute and relative tests on the matching statistics. The resulting y-parallaxes were converted into preliminary cloud heights after Prata and Turner (1997), considering that the zenith angles have to be projected on the along-track plane. From the x-parallaxes, the cross-track motion component was computed. For the final cloud-top heights, the preliminary heights were then corrected by the along-track motion error, with the along-track motion component from Meteosat-8. For MISR triplets (BF-AN-DF, with BF as template image), the final cloud heights, along- and cross-track motion components were additionally calculated with the linear equations described in Diner et al. (1999) and

Horvath and Davies (2001). For visualization, the height and motion values of the successfully matched points are finally interpolated with triangulation to a regular grid.

For Meteosat-5/-7 and Meteosat-5/-8 HRV, 3 pyramid levels were used. Before matching, the images were preprocessed with a Wallis filter for contrast enhancement. The corresponding points in the image sequence were then determined with the MPGC matching algorithm. For the Meteosat-5 and Meteosat-7 combination, it is a near-simultaneous two-view matching. For the Meteosat-5 and Meteosat-8 HRV combination, three images were used in the matching, 1) Meteosat-5 with nominal image start time t (e.g. 06:30), 2) Meteosat-8 HRV with image start time t (e.g. 06:30), and 3) Meteosat-8 HRV with image start time $t+15$ min (e.g. 06:45). Figure 4 shows an example of this triplet matching process for Meteosat-5 and two Meteosat-8 HRV images (template: Meteosat-8 HRV image at time t). The CTW was only calculated for the Meteosat-5/Meteosat-8 HRV combination, from the x- and y-disparities between Meteosat-8 HRV at time t and Meteosat-8 HRV at time $t+1$. For the CTH retrieval, the zenith angles are calculated from the acquisition geometry. Several assumptions had to be made for Meteosat-5 and Meteosat-7, as the satellite position and acquisition time is only known at image start and end. The acquisition time t_{pixel} of a pixel was approximated by linear interpolation between image start and end time, with the line number from the rectified image. Due to the rather large inclination of Meteosat-5 (i.e. 6.3°) and the deviations of the SSP from its nominal position (which is used for the georectification), this is a quite rough approximation, which should clearly be improved. The satellite position was then approximated by linear interpolation between the satellite position at image start and at image end, using the approximate acquisition time t_{pixel} . As further assumption (similar to MISR), the CTH and CTW within the 15-minute interval were taken as constant, with no vertical cloud motion component.

3.3 Error analysis

The accuracy of the retrieved cloud-top heights and winds with stereo-photogrammetric methods is largely influenced by the geometric configuration (base-to-height ratio B/H , time difference Δt) and by the matching accuracy. The MPGC LSM matching algorithm is well known for its high accuracy and reliability. In the case of clouds, the theoretical accuracy σ of the matching is about ± 0.5 pixels, which is of course worse than for



Figure 4. MPG triplet matching between Meteosat-8 HRV at 06:34 UTC (left), Meteosat-8 HRV at 06:49 UTC (center) and Meteosat-5 at 06:37 UTC (right). The template and patch windows are shown in green and red, respectively. It can be seen that there are larger differences in the cloud structures between Meteosat-8 HRV at 06:34 (left) and at 06:49 (center), due to changes within the 15-minute time interval.

e.g. signaled points. Table 1 summarizes the estimated accuracies of stereo cloud-top height and motion from MISR and Meteosat-5/8 HRV. It is important to note that these theoretical accuracies only include the geometric configuration and the matching accuracy, but no systematic errors which could occur (e.g. geolocation errors, angle/time errors, etc.).

Sensor	Pixel size [m]	B/H	Δt [s]	CTH accuracy [m]	Along-track motion accuracy [m/s]
MISR AN_AF (M8 wind correction)	275	0.49	46	340	-
MISR BF_AN_DF		1.02; 1.83	91; 112	600	5.6
Meteosat-5/-8 HRV	2500 (M5), 1100 (M8)	1.4 - 2.5	600	1200 (at 0° N 30° E)	2.0

Table 1. Theoretical accuracies of the stereo CTH retrieval from MISR AN_AF, MISR BF_AN_DF and Meteosat-5/Meteosat-8 HRV, assuming a measurement accuracy of ± 0.5 pixels for MISR and ± 1.0 HRV pixels for Meteosat-5/-8.

The geometric accuracy determines how well the look vectors intersect in the CTH calculation. The geometry of each look vector is influenced by the apparent position of the cloud feature on the ground (i.e. reference ellipsoid) and by the satellite position. Due to cloud motion, the acquisition time additionally influences the look vector geometry in non-simultaneous multi-view CTH retrievals. For the Meteosat satellites, the accuracy of these three factors – geolocation, satellite position and acquisition time – is different for the MFG and MSG satellites. For MFG, the satellite position is only given at image start and end time. In terms of the acquisition time, only the nominal image start time and nominal scan rate are known, i.e. no actual acquisition times. The geolocation is accurate to about 1-2 VIS pixels, i.e. 2.5-5.0 km at the SSP. For MSG, the available geometric information is much improved. The satellite position can be calculated from an orbit polynomial given in the image header, using the exact acquisition time. The actual acquisition time of each pixel is still not known, but the average acquisition time for each line is given in the rectified L1.5 product. The geolocation optimization is currently in progress to reach the requirements of 0.5-1.0 pixels for HRV, i.e. 0.5-1.0 km at the SSP. Unfortunately, the current absolute Meteosat-8 HRV geolocation is only accurate to about 1.0-2.0 HRV pixels, i.e. 1.0-2.0 km at the SSP. For MISR, the geometric accuracy is rather high, with an absolute geolocation of all views of 0.5-1.0 pixels, i.e. 140-275 m, except the Da camera, and detailed informations about the satellite position and exact acquisition time of each pixel.

Another error source which has also to be considered in this analysis is the validity of the assumptions. As described above, it is assumed that the CTH and CTW within the 15-minute interval are constant, with no vertical cloud motion component. So, stereo CTH errors can likely occur in regions with strong vertical cloud

motion. Furthermore, the area-based MPGC least-squares matching assumes that a point within a locally smooth surface is matched, which is of course not always fulfilled within clouds, especially at cloud layer discontinuities or at cloud borders.

4. RESULTS

Stereo height retrieval was tested within two target areas of the 26-Dec-2003 images. Target area 1 was centered at (22 S | 51 E), within MISR Path 156, and target area 2 at (5 S | 30 E), within MISR Path 172. In Table 2, the detailed acquisition times (nominal time for Meteosat-5 and Meteosat-7, actual time for MISR and Meteosat-8) are listed.

Scene	MISR	Meteosat-5	Meteosat-7	Meteosat-8	Meteosat-8
26-12-2003, Path 156, blocks 107-110 (22 S 51 E)	AN: 06:53:26	06:37:11	06:37:30	06:33:43	06:48:43
26-12-2003, Path 172, blocks 93-96 (5 S 30 E)	AN: 08:27:28	08:11:18	08:11:18	08:05:36	08:22:36

Table 2. Acquisition times (UTC) of MISR, Meteosat-5, Meteosat-7 and Meteosat-8 HRV on 26/12/2003.

The Meteosat-5 and Meteosat-8 image combination for target area 2 is shown in Figure 5. The matching within the image triplets was successful for most points. Of course, some points failed in the matching due to disappearance of cloud structures or appearance of new features within the 15-minute time interval. However, the matching results look promising, with an estimated accuracy of about ± 0.5 -2.0 MISR SOM pixels. Further analysis of the matching results and detailed comparison with the MISR CTH results will help to further quantify the matching accuracy between the new Meteosat-8 HRV and Meteosat-5 images.

The comparison of the stereo CTH from Meteosat-8 HRV/Meteosat-5 with the MISR stereo CTH (from MISR L1B2 data) show considerably large differences, compared with the rather small differences between the MISR L1B2 and the operational NASA-JPL MISR L2TC stereo heights (Figure 6). It has to be analyzed in detail which factors are mainly contributing to these differences. The largest errors in the Meteosat-8 HRV/Meteosat-5 stereo CTHs are most likely introduced by the geolocation inaccuracies explained in Section 3. Further error sources are the acquisition geometry, the validity of the retrieval assumptions and the definition accuracy (i.e. are the same cloud features matched with M8/M5 as with MISR).

Stereo CTH on a 1.1 x 1.1 km grid and CTW on a 70.4 x 70.4 km grid are also provided within the operational MISR processing chain as part of the level 2TC product. The L2TC stereo CTH raw winds product for the same scene is shown in Figure 6 right. Important to note is that, due to processing time constraints, no subpixel matching algorithm is used. The L2TC results are not retrieved simultaneously, but in two steps: 1) triplet retrieval of 1-2 CTW values which are representative for the CTW within a 70.4 x 70.4 km box (i.e. first and second peak in histogram) and 2) preliminary CTH retrieval from AN-AF stereo pair for each 275 x 275 m pixel, averaging of the results to the 1.1 x 1.1 km grid and finally correction of these preliminary CTHs with the CTW box values from step 1. The advantage of the L2TC algorithm is the use of a histogram analysis over several hundred triplet matches within each 70.4 x 70.4 km box, which allows to

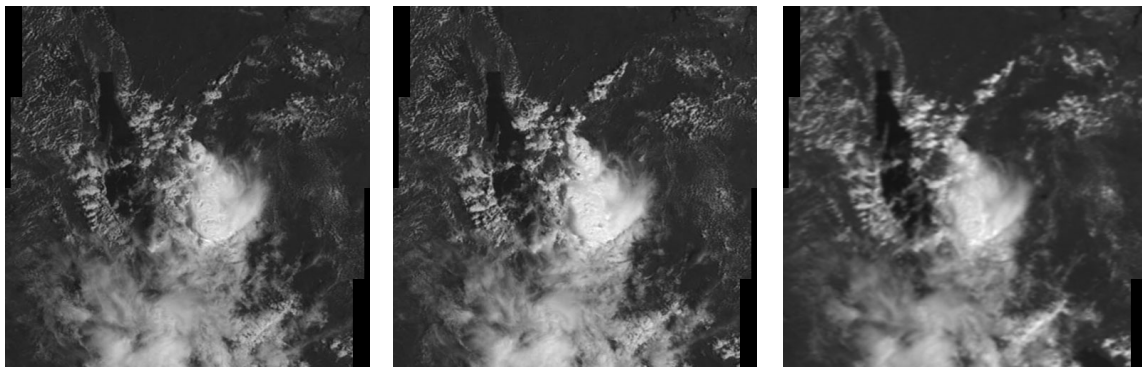


Figure 5. Meteosat-8 HRV image on 26-Dec-2003 at 08:05:36 UTC (left), Meteosat-8 HRV image at 08:22:36 UTC (center) and Meteosat-5 image at 08:11:18 UTC.

retrieve a rather consistent CTW field at this resolution. The grid resolution could also be increased, e.g. to 37.2 x 37.2 km, as was shown in Horvath et al. (2002). However, the disadvantage of this method is the use of the coarse boxes for the CTW retrieval, which usually introduces artificial discontinuities in the high-resolution CTH field at grid borders (see Figure 6 right). Prior segmentation of the cloud structures would be a promising alternative, allowing both a histogram analysis to reduce the standard deviation of the along-track wind component and a more consistent CTH correction.

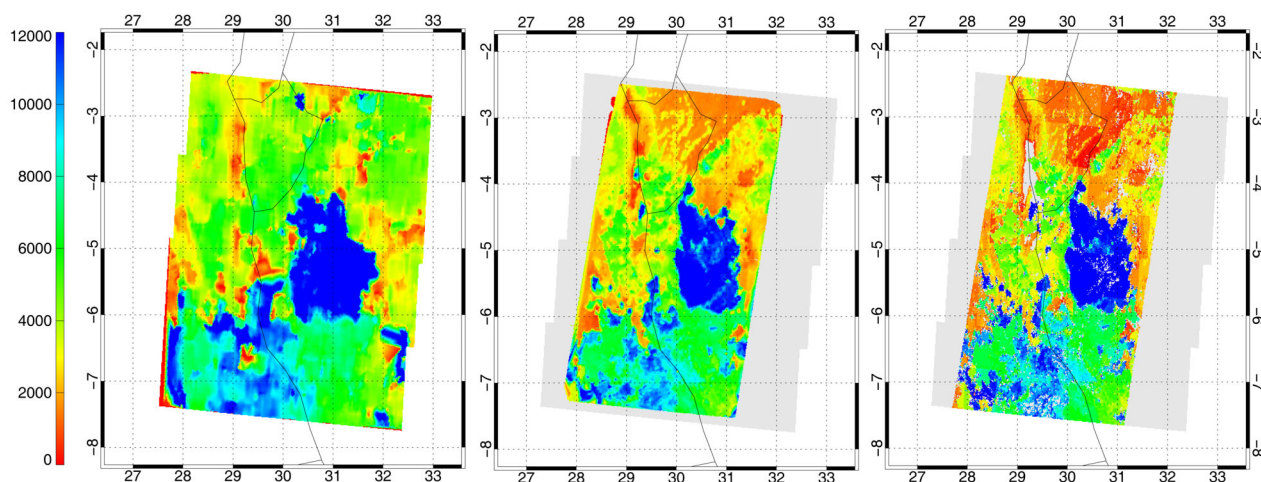


Figure 6. Stereo CTH results on 26-Dec-2003 at 08:00, MISR Path 172, from Meteosat-8/-5 (left), MISR L1B2 (center) and MISR L2TC (right).

5. CONCLUSIONS AND OUTLOOK

In this paper, the possibilities of stereo height retrievals from the currently operational Meteosat satellites have been analyzed. In particular, the new Meteosat-8 HRV and Meteosat-5 combination has been tested. The absolute and relative geolocation, viewing angle and acquisition time characteristics of each Meteosat satellite have been studied. To account for the time difference between the Meteosat-8 HRV and Meteosat-5 acquisition, two subsequent Meteosat-8 HRV images were taken. The cloud advection effect was then corrected by tracking of these two subsequent HRV images. From the first results, it seems as if the time difference between Meteosat-8 and Meteosat-5 is no problem for the stereo CTH accuracy, except if there are large CTH changes or strong vertical motion within the time interval of 15 minutes. While the triplet matching tests between two Meteosat-8 HRV images and the corresponding Meteosat-5 image showed to perform quite well, the information about the acquisition time and satellite position (in particular MFG satellites), as well as the geolocation accuracy are not good enough for an accurate stereo CTH retrieval between Meteosat-5 and Meteosat-8 HRV. Local improvement of the geolocation with near coast lines is often impossible due to cloud cover. We will have to analyze the spatial structure of the geolocation errors in more detail, for an improvement of the ground (i.e. ellipsoid) coordinates in the CTH estimation. Better knowledge of the exact acquisition time of a cloud point will be hopefully obtained by including an additional field in the Meteosat MFG header in the near future. By achieving a measurement accuracy from the matching of ± 0.5 HRV pixels and a geolocation accuracy of about ± 0.5 -1.0 HRV pixels, the final goal of a stereo CTH accuracy of about ± 1 km should be feasible. The stereo heights from Meteosat-8 HRV and Meteosat-5 would then represent a good validation method for the other Meteosat-8 height assignment techniques. Further quantitative comparisons of the M5/M8 stereo heights will be done with MISR L1B2 and MISR L2TC CTHs, as well as with coincident MODIS and MERIS CTP products, within the Eumetsat CTH comparison study to identify the contribution of the various error sources mentioned in Section 3.3.

ACKNOWLEDGEMENTS

The Meteosat data were received from the EUMETSAT MARF Archive Facility and the MISR data were obtained from the NASA Langley Research Center Atmospheric Sciences Data Center. This work is funded by the Bundesamt für Bildung und Wissenschaft (BBW) within the EU-project CLOUDMAP2 (BBW Nr. 00.0355-1) and EUMETSAT. G. Seiz would like to thank Stephen Tjemkes and Johannes Schmetz for the organization of the scientific visit at EUMETSAT in April 2004. Furthermore, the comments and advices from Marco Clerici, Greg Dew, Yves Govaerts, Chris Hanson, Akos Horvath, Ken Holmlund, Marianne Koenig,

Hans-Joachim Lutz, Catherine Moroney, Daniela Poli, Arthur de Smet and Bogdan Teianu are thankfully acknowledged.

REFERENCES

- BALTSAVIAS, E.P. (1991). Multiphoto Geometrically Constrained Matching. Ph.D. dissertation, Institute of Geodesy and Photogrammetry, ETH Zurich, Mitteilungen No. 49, 221 p.
- CAMPBELL, G., HOLMLUND, K. (2000). Geometric cloud heights from Meteosat and AVHRR. In Proc. Fifth International Winds Workshop, EUM P28.
- CAMPBELL, G., HOLMLUND, K. (2004). Geometric cloud heights from Meteosat. *Int. J. Rem. Sens.* (in press).
- DINER, D., DAVIES, R., DI GIROLAMO, L., HORVATH, A., MORONEY, C., MULLER, J.-P., PARADISE, S., WENKERT, D., AND ZONG, J. (1999). MISR Level 2 Cloud Detection and Classification. JPL Technical Report ATBD-MISR-07.
- FISCHER, J., PREUSKER, R., SEIZ, G., POLI, D., GRUEN, A., POULSEN, C., MUTLOW, C., TJEMKES, S., BORDE, R., DE SMET, A., 2004. Validation of cloud top pressure derived from MSG-SEVIRI observations through a comparison with independent observations. EUMETSAT Users' Conference, Prague.
- FÖRSTNER, W., GÜLCH, E. (1987). A fast operator for detection and precise location of distinct points, corners, and centers of circular features. Proc. ISPRS Intercommission Conf. on Fast Processing of Photogrammetric Data, Interlaken, Switzerland, 2-4 June, pp. 281-305.
- FUJITA, T. (1982). Principle of stereoscopic height computations and their applications to strato-spheric cirrus over severe thunderstorms. *J. Met. Soc. Japan*, **60**, 1, pp. 355-368.
- GRUEN, A. (1985). Adaptive least squares correlation: a powerful image matching technique. *S. Afr. J. of Photogrammetry, Remote Sensing and Cartography*, **14**, 3, pp. 175-187.
- HASLER, F. (1981). Stereographic observations from geosynchronous satellites: an important new tool for the atmospheric sciences. *Bull. Am. Met. Soc.*, **62**, 2, pp. 194-212.
- HORVATH, A., DAVIES, R. (2001). Feasibility and error analysis of cloud motion wind extraction from near-simultaneous multiangle MISR measurements. *J. Atmos. Ocean. Technology*, **18**, 4, pp. 591-608.
- HORVATH, A., DAVIES, R., SEIZ, G. (2002). Status of MISR cloud-motion wind product. Proc. 6th International Winds Workshop, Madison, Wisconsin, USA, 7-10 May, Eumetsat publication EUM P35, Eumetsat, Darmstadt, Germany.
- LEWICKI, S., CHAFIN, B., CREAN, K., GLUCK, S., MILLER, K., AND PARADISE, S. (1999). MISR data products specifications. JPL Technical report.
- PRATA, A.J., TURNER, P.J. (1997). Cloud-top height determination using ATSR data. *Rem. Sens. Env.*, **59**, 1, pp. 1-13.
- SEIZ, G., BALTSAVIAS, E.P. (2000). Satellite- and ground-based stereo analysis of clouds during MAP. EUMETSAT Conference Proceedings, Bologna, pp. 805-812.
- SEIZ, G., BALTSAVIAS, E.P., GRUEN, A. (2001). Comparison of satellite-based cloud-top height and wind from MISR, ATSR2 and Meteosat-6 Rapid Scans. EUMETSAT Users' Conference, Antalya, 1-5 October 2001. EUMETSAT Conference Proceedings, pp. 224-230.
- SEIZ, G. (2003). Ground- and satellite-based multi-view photogrammetric determination of 3D cloud geometry. Ph.D. thesis, Institute of Geodesy and Photogrammetry, ETH Zuerich, June 2003. IGP Mitteilungen Nr. 80.
- SEIZ, G., BALTSAVIAS, E.P., GRUEN, A. (2003). High-resolution cloud motion analysis with Meteosat-6 Rapid Scans, MISR and ASTER. EUMETSAT Meteorological Satellite Conference, Weimar, pp. 352-358.
- WALLIS, R. (1976). An approach to the space variant restoration and enhancement of images. Proc. of Symp. on Current Mathematical Problems in Image Science, Naval Postgraduate School, Monterey CA.
- YI, H., MINNIS, P., NGUYEN, L., DOELLING, D. (2001). A proposed multiangle satellite dataset using GEO, LEO and Triana. In Proc. 11th AMS Conference on Satellite Meteorology and Oceanography.